



HAL
open science

A Comprehensive Code-to-Code Comparison Study with the Modified IEA15MW-UMaine Floating Wind Turbine for H2020 HIPERWIND Project

Taeseong Kim, Anand Natarajan, Anaïs Lovera, Emricka Julan, Christophe Peyrard, Matteo Capaldo, Guillaume Huwart, Pauline Bozonnet, Martin Guiton

► To cite this version:

Taeseong Kim, Anand Natarajan, Anaïs Lovera, Emricka Julan, Christophe Peyrard, et al.. A Comprehensive Code-to-Code Comparison Study with the Modified IEA15MW-UMaine Floating Wind Turbine for H2020 HIPERWIND Project. *Journal of Physics: Conference Series*, 2022, 2265 (4), pp.042006. 10.1088/1742-6596/2265/4/042006 . hal-03734978

HAL Id: hal-03734978

<https://ifp.hal.science/hal-03734978>

Submitted on 21 Jul 2022

HAL is a multi-disciplinary open access archive for the deposit and dissemination of scientific research documents, whether they are published or not. The documents may come from teaching and research institutions in France or abroad, or from public or private research centers.

L'archive ouverte pluridisciplinaire **HAL**, est destinée au dépôt et à la diffusion de documents scientifiques de niveau recherche, publiés ou non, émanant des établissements d'enseignement et de recherche français ou étrangers, des laboratoires publics ou privés.



Distributed under a Creative Commons Attribution 4.0 International License

PAPER • OPEN ACCESS

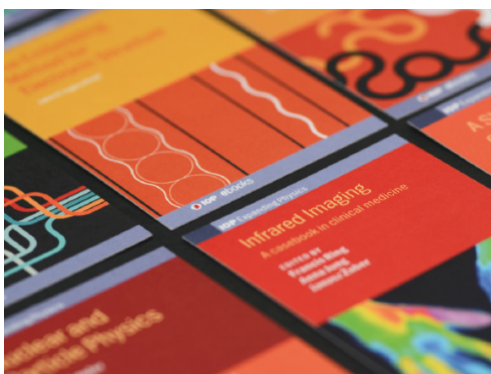
A comprehensive code-to-code comparison study with the modified IEA15MW-UMaine Floating Wind Turbine for H2020 HIPERWIND project

To cite this article: Taeseong Kim *et al* 2022 *J. Phys.: Conf. Ser.* **2265** 042006

View the [article online](#) for updates and enhancements.

You may also like

- [Upscaling and levelized cost of energy for offshore wind turbines supported by semi-submersible floating platforms](#)
Yuka Kikuchi and Takeshi Ishihara
- [Integrated design of a semi-submersible floating vertical axis wind turbine \(VAWT\) with active blade pitch control](#)
Fons Huijs, Ebert Vlasveld, Maël Gormand et al.
- [3D printed self-propelled composite floaters](#)
Soheila Shabaniverki, Antonio Alvarez-Valdivia and Jaime J. Juárez



IOP | ebooks™

Bringing together innovative digital publishing with leading authors from the global scientific community.

Start exploring the collection—download the first chapter of every title for free.

A comprehensive code-to-code comparison study with the modified IEA15MW-UMaine Floating Wind Turbine for H2020 HIPERWIND project

Taeseong Kim¹, Anand Natarajan¹, Anaïs Lovera², Emricka Julan², Christophe Peyrard³, Matteo Capaldo², Guillaume Huwart⁴, Pauline Bozonnet⁵, Martin Guiton⁵,

¹DTU Wind Energy, Frederiksborgvej 399, 4000, Roskilde, Denmark

²EDF Lab Saclay, 7 bv. Gaspard Monge, 91120 Palaiseau, France

³EDF Lab Chatou, 6 Quai Watier, 78400 Chatou, France

⁴IFP Energies nouvelles, 1 et 4 avenue de Bois-Préau, 92852, France

⁵IFP Energies nouvelles, Rond-point de l'échangeur de Solaize, BP 3, 69360, France

Author contact email: tkim@dtu.dk

Keywords: FOWT, aero-servo-hydro-elastic model, benchmark, IEA 15MW, semi-submersible

Abstract: An extensive code-to-code comparison among DIEGO, DLW and HAWC2 has been performed on a floating wind turbine (modified version of UMaine floater with IEAWIND 15MW wind turbine). In total, 10 cases are compared, and a few key results of this comparison are reported in this paper. From the comparisons, it is clearly seen that the results predicted by the three codes are generally agreed well despite some differences in specific degrees of freedom like roll, sway and yaw for the extreme load case, which requires additional investigations.

1. Introduction

The European Commission has set an ambitious target of up to 450 GW of offshore wind by 2050 [1]. With offshore wind power set to form the backbone of green electricity production in Europe, there is an urgent need for cost-effective realization of the reliability of major wind turbine components, especially for floating offshore wind turbines (FOWTs). HIPERWIND H2020 project [2] aims at contributing to this objective by modelling the entire chain from environmental conditions to wind farm design for uncertainty reduction and to increase reliability. As the first step of this project, this paper presents an extensive code-to-code comparison of the model response from three different aero-servo-hydro-elastic numerical tools (DIEGO, DeepLines WindTM (DLW) and HAWC2). The compared model is the modified IEA15MW/UMaine floating wind turbine [3]. In total 10 test cases are considered to compare the responses.

2. Methodology

The methodology employed herein is similar to the OC6 (Offshore Code Comparison Collaboration Continued, with correlation and uncertainty) project of IEA Wind Task30, which also concerns code-



Content from this work may be used under the terms of the [Creative Commons Attribution 3.0 licence](https://creativecommons.org/licenses/by/3.0/). Any further distribution of this work must maintain attribution to the author(s) and the title of the work, journal citation and DOI.

to-code comparison [4]. A stepwise comparison procedure is performed. Detailed test cases are summarized in Table 1. The model complexity is increased step-by-step to identify potential modelling discrepancies introduced by different assumptions or model implementations in the various codes.

Table 1: List of test cases

| Test case # | Test case description |
|-------------|---|
| 1 | Free decay test - No wind and wave, Apply and then release an initial displacement and rotation in Heave, Surge, Pitch and Yaw directions |
| 2 | Pull out test - No wind and wave, Impose displacement on the floater in Surge direction |
| 3 | Wind step – From 3 to 25 m/s with 1 m/s step at hub height, Wind shear (power law: $\alpha=0.2$), no turbulence. |
| 4 | Regular wave test – No wind, Idling condition with 90° blade pitch, 3 different regular waves ($H = 2$ m and $T = 6, 10, \text{ and } 16$ seconds). |
| 5 | Irregular wave test – No wind, Idling condition with 90° blade pitch, 2 different JONSWAP spectrum cases with Wheeler stretching model ($H_s = 2$ m, $T_p = 7$ s, $\gamma=3$ and $H_s = 13$ m, $T_p = 16$ s, $\gamma=1$). |
| 6 | Normal shutdown – No wave |
| 7 | Shutdown with extreme gust – No wave |
| 8 | Turbulent wind without wave – 8 m/s and 15 m/s |
| 9 | Parked condition without yaw error – Rotor blocked with 90° blade pitch, wind speed at 50 m/s, JONSWAP spectrum with Wheeler stretching model ($H_s = 13$ m, $T_p = 16$ s, $\gamma = 1$). |
| 10 | Parked condition with extreme yaw error ($\pm 30^\circ$) – Rotor blocked with 90° blade pitch, wind speed at 50m/s, JONSWAP spectrum with Wheeler stretching model ($H_s = 13$ m, $T_p = 16$ s, $\gamma = 1$). |

In this study, the floating system used is based on the IEA 15MW turbine defined in [5] and the semi-submersible foundation proposed by the University of Maine [3]. From [3], the first tower natural frequencies are reported to be around 0.48 Hz. However, it was investigated that the first natural frequencies of the tower dropped around 0.39-0.40 Hz when hydrodynamic added mass is considered in the modal analysis. This value is closer to the 3P frequency of the FOWT (about 0.375Hz at the rated rotational speed). In this study, to avoid resonance excitations due to the lowered natural frequency of the tower, a new tower design that provides a safe distance from the 3P frequency (about 15% of 3P frequency) is introduced, whereby the total tower weight is increased from 1263 tons to 1515 tons. Manufacturing constraints are also considered, such as diameter and thickness ratio lower than 200 to avoid local buckling and maximum sectional angle variation of 3 degrees. This leads to other modifications on the weight of the nacelle and on the ballast in the floater to have a very small variation in the total mass and keep the draft of the FOWT unchanged. All the floater geometrical parameters have been kept unchanged, and only the ballast has been modified. Furthermore, in this study, the target offshore site is South Brittany (France) with a water depth of 150m instead of 200m which is the original design. Thus, it requires additional modifications for the ballast and the mooring. Three different numerical tools, HAWC2, DIEGO and DLW, were used for a comprehensive benchmark loads study. HAWC2 (Horizontal Axis Wind turbine simulation Code 2nd generation) is a state-of-the-art aero-servo-hydro-elastic analysis tool developed by DTU Wind Energy [6-8]. DIEGO (Dynamique Intégrée des Eoliennes et Génératrices Offshore) is an in-house aero-hydro-servo-elastic code developed by EDF R&D. DeepLines WindTM (DLW) is a state-of-the-art aero-servo-hydro-elastic analysis tool based on Finite Element Analysis and developed by Principia and IFP Energies Nouvelles, to assess the dynamic response of floating and fixed-bottom wind turbines submitted to offshore environmental loadings [9].

To solve the diffraction-radiation problem and to generate hydrodynamic databases, each numerical tool uses a different solver. HAWC2 obtains its hydrodynamic database from WAMIT. DIEGO uses the open source solver NEMOH, developed by Ecole Centrale de Nantes. DLW relies on Principia

software DIODORETM. The hydrodynamic databases are limited to the first order in the present benchmark. The second-order wave loads from the diffraction-radiation (QTF) have not been computed and used for the time-domain simulations. However, the drag forces coming from the Morison elements are expected to produce a small level of nonlinear loads. These loads could be able to generate drift forces, depending on the strategies used by the different partners for drag (additional specific elements carrying these drag forces for DLW and DIEGO while HAWC2 uses a quadratic damping matrix). At the end, this difference in the drag excitation is regarded as negligible in most of the cases.

3. Results

In this paper, some of the key results will be presented based on the considered test cases defined in Table 1.

3.1. *Modal analysis*

Initially, the location of the full system (turbine and floater) center of gravity is compared among the three codes. It can be noted that this location does not account for the mooring lines. Table 2 shows the coordinates of the complete turbine center of gravity computed by the three codes. It can be concluded that the three tools show a good agreement although HAWC2 predicts the center of gravity slightly higher.

Table 2: Center of gravity of the entire floating system (except mooring lines)

| | X | Y | Z |
|-------|---------|--------|---------|
| DLW | -0.32 m | 0.00 m | -2.38 m |
| DIEGO | -0.32 m | 0.00 m | -2.27 m |
| HAWC2 | -0.33 m | 0.00 m | -2.03 m |

Modal analysis, free decay test and regular wave test results are presented. The first modes are compared. The modal analysis in the floating configuration allows comparing floater, tower, and blade modes. Table 3 shows that all modes are well corresponding for all three numerical tools.

Table 3: First modes of the entire floating system

| | DLW (Hz) | DIEGO (Hz) | HAWC2 (Hz) |
|-----------------------|----------|------------|------------|
| Surge | 0.007 | 0.007 | 0.007 |
| Sway | 0.007 | 0.007 | 0.007 |
| Heave | 0.050 | 0.050 | 0.050 |
| Roll | 0.036 | 0.036 | 0.036 |
| Pitch | 0.036 | 0.036 | 0.036 |
| Yaw | 0.009 | 0.009 | 0.009 |
| 1 st tower | 0.460 | 0.427 | 0.455 |
| 2 nd tower | 0.465 | 0.448 | 0.465 |
| Blade | 0.524 | 0.535 | 0.521 |

3.2. *Free decay test*

Four decay tests in different directions without wind and waves are performed. These decay tests apply an initial displacement (or rotation) on the floater, set the floater free and then observe the displacement (or rotation) at the keel. Figure 1(a) depicts the time series of the surge motion for the decay test in which initially a displacement of 10m in the surge direction is applied. It can be seen that the three codes are in good agreement, with a decrease of the surge motion very similar among the three time series. Figure 1(b) shows the PSD of the surge motion. A peak is observed at the surge floater frequency (i.e. 0.007 Hz), another peak around 0.036 Hz (i.e. pitch - frequency) is also seen.

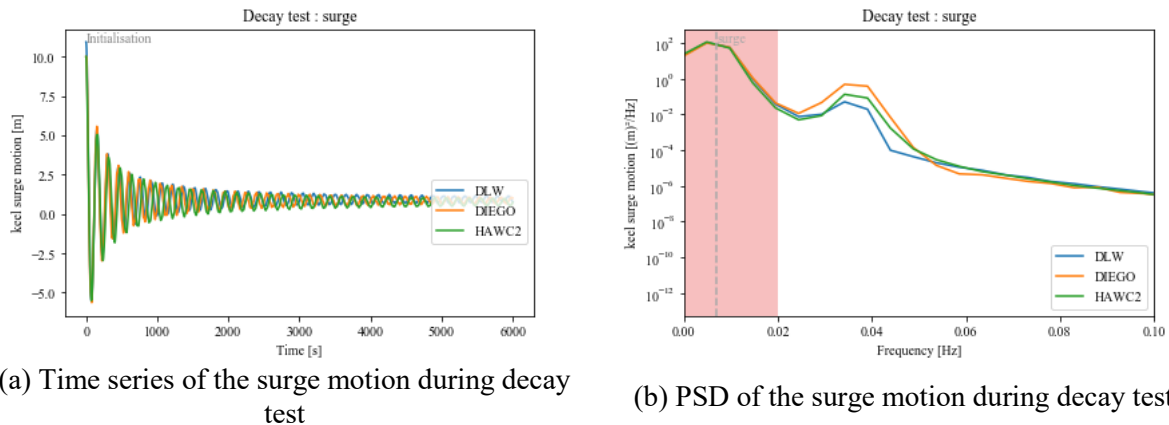


Figure 1: The surge motion during decay test

3.3. *Wind step case*

A wind step simulation has been performed to validate controller behaviours. Figure 2 shows the time series of the wind speed. The initialization duration is marked with a grey rectangle that refers to the first 200 seconds of the simulation. Wind speed is increased as a step from 4 m/s to 25 m/s. Each wind step is changed within 1s and maintained during 100s.

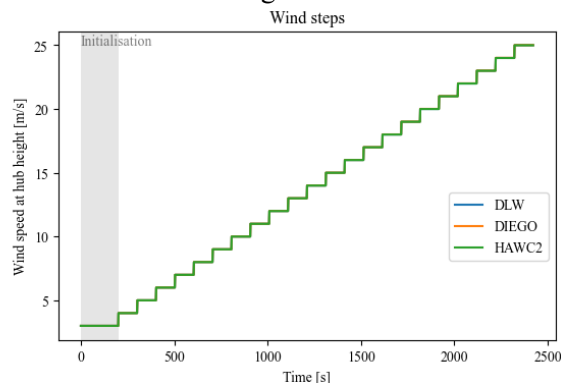
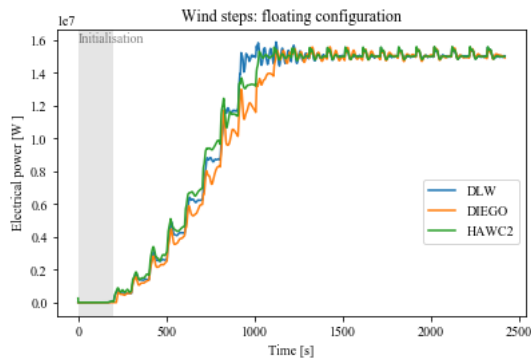


Figure 2: Wind speed at hub height time series considered in the wind steps simulations

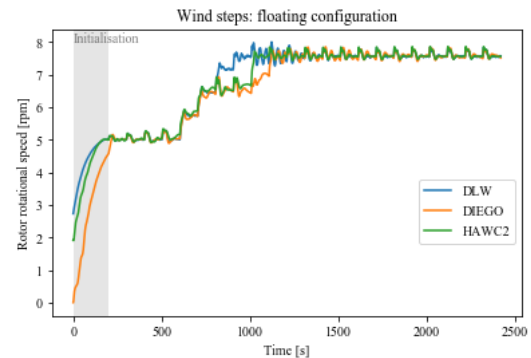
It must be noted that DTU, IFPEN and EDF have a different control strategy:

- HAWC2 uses its own blade pitch controller, whereas the ROSCO controller is used only for the generator torque control.
- DLW uses the ROSCO controller with a modification in the pitch saturation limits in order to accommodate a different choice in the blade elastic model.
- DIEGO uses the ROSCO controller with the input parameters as provided by NREL and UMaine.

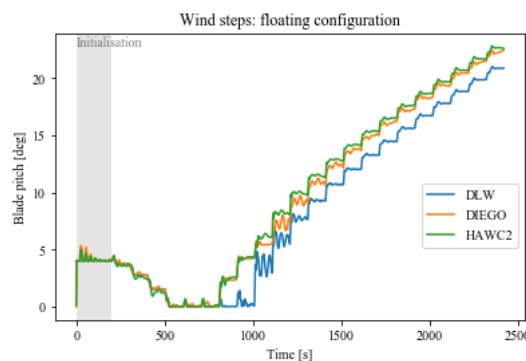
Figure 3 shows the electrical power, rotational speed and blade pitch during the wind step case. As expected, the evolution of those quantities is very similar, which proves that the floating specific feedback control is working properly. The rated power and rotor speed are obtained for a lower wind speed by DLW because of the differences in the model corresponding to the BeamDyn blade version instead of the ElastoDyn one.



(a) Electrical power during the wind steps



(b) Rotor rotational speed during the wind steps

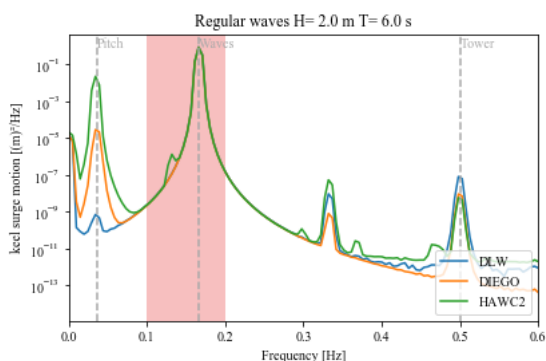


(c) Blade pitch during the wind steps

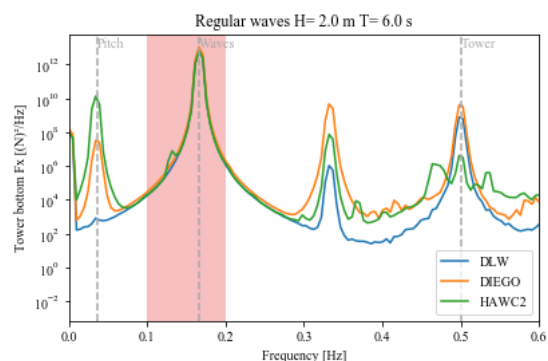
Figure 3: Floating wind turbine system responses for wind step case

3.4. *Wave only load cases*

In total, three load cases considering regular wave conditions were performed. In this section only the regular wave considering $H=2$ m and $T=6$ s is shown. Figures 4 (a) and (b) show the PSD of the surge motion and the bending moment at tower bottom. It can be noted that the three codes are in very good agreement for this peak. The y-scale in the PSD plots is logarithmic.



(a) PSD of the surge motion



(b) PSD of the force at tower bottom

Figure 4: The surge motion and tower bottom force during regular wave case ($H=2$ m and $T=6$ s)

3.5. *Irregular wave load cases*

In total, two load cases considering irregular waves conditions were performed. The irregular wave conditions are given by the following JONSWAP parameters, 1) $H_s=2$ m, $T_p=7$ s and $\gamma=3$ and 2)

$H_s=13$ m, $T_p=16$ s and $\gamma=1$. In this section only the irregular wave considering $H_s=13$ m, $T_p=16$ s and $\gamma=1$ is shown. Figure 5 shows the PSD of the wave elevation.

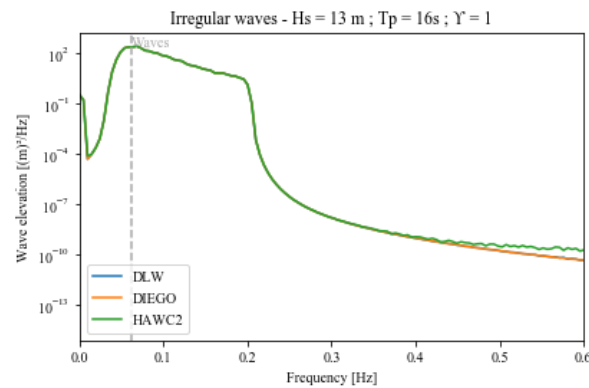


Figure 5: PSD of the wave elevation ($H_s = 13$ m, $T_p = 16$ s and $\gamma = 1$)

Table 4 summarizes the basic statistics of various quantities of interest. Overall, the motion statistics for all DoFs show good agreement between the three codes. DLW produces however a higher mean surge which is related to a strong decrease in the tension of mooring line 1. The low minimum value of the tension force on the mooring line #1 (FT1) actually indicates that the model is not well designed against such extreme waves. HAWC2 produces a lower mean surge because it considers no Morison excitation. The dynamic pitch response is a bit lower than DIEGO and DLW, but this seems to have little effect on the moment at tower bottom which is well aligned with DLW. Mooring tension forces predicted from the three codes are in good agreement for line 2 (FT2) and 3 (FT3). But significant difference for the line 1 standard deviation is observed, DIEGO being 17% under DLW and HAWC2 33% above DLW. The highly non-linear dynamics when a mooring line tension is not high enough should explain this discrepancy. Forces in the tower, F_x , are well aligned for the three codes regarding the standard deviation.

Table 4: Basic statistics of quantities of interest for irregular wave simulation ($H_s = 13$ m, $T_p = 16$ s and $\gamma = 1$)

| surge [m] | Mean | Maximum | Minimum | Standard deviation |
|-----------|-------|---------|---------|--------------------|
| DLW | 3.85 | 20.48 | -2.62 | 2.53 |
| DIEGO | 2.24 | 12.26 | -5.65 | 2.53 |
| HAWC2 | 1.12 | 9.59 | -6.07 | 2.48 |
| sway [m] | Mean | Maximum | Minimum | Standard deviation |
| DLW | 0.00 | 0.00 | -0.01 | 0.00 |
| DIEGO | 0.00 | 0.05 | -0.06 | 0.02 |
| HAWC2 | 0.00 | 0.02 | -0.02 | 0.01 |
| heave [m] | Mean | Maximum | Minimum | Standard deviation |
| DLW | -0.10 | 5.98 | -7.03 | 1.77 |
| DIEGO | -0.17 | 5.75 | -6.85 | 1.82 |
| HAWC2 | -0.01 | 4.50 | -4.40 | 1.46 |
| roll [°] | Mean | Maximum | Minimum | Standard deviation |
| DLW | 0.00 | 0.015 | -0.01 | 0.00 |
| DIEGO | 0.00 | 0.06 | -0.07 | 0.02 |
| HAWC2 | 0.00 | 0.01 | -0.01 | 0.00 |
| pitch [°] | Mean | Maximum | Minimum | Standard deviation |
| DLW | -1.55 | 1.47 | -5.43 | 0.94 |
| DIEGO | -1.39 | 1.09 | -4.61 | 0.85 |
| HAWC2 | -1.42 | 0.41 | -3.67 | 0.59 |

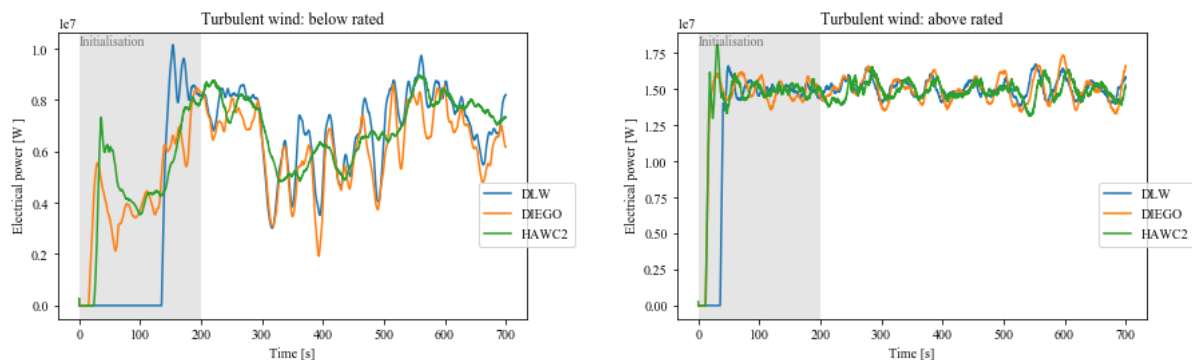
| yaw [°] | Mean | Maximum | Minimum | Standard deviation |
|----------------|---------|---------|---------|--------------------|
| DLW | 0.01 | 0.03 | 0.009 | 0.00 |
| DIEGO | 0.01 | 0.06 | -0.02 | 0.01 |
| HAWC2 | 0.00 | 0.02 | -0.01 | 0.00 |
| Fx [MN] | Mean | Maximum | Minimum | Standard deviation |
| DLW | 0.00 | 3.86 | -3.50 | 0.93 |
| DIEGO | -0.01 | 2.90 | -3.47 | 0.82 |
| HAWC2 | 0.00 | 3.87 | -3.34 | 0.89 |
| My [MN.m] | Mean | Maximum | Minimum | Standard deviation |
| DLW | -119.09 | 288.07 | -602.82 | 112.97 |
| DIEGO | -100.97 | 79.33 | -319.32 | 49.23 |
| HAWC2 | -114.12 | 227.99 | -460.12 | 94.23 |
| FT1 [MN] | Mean | Maximum | Minimum | Standard deviation |
| DLW | 1.72 | 2.44 | 0.66 | 0.12 |
| DIEGO | 1.67 | 2.10 | 1.27 | 0.08 |
| HAWC2 | 1.49 | 2.40 | 0.27 | 0.14 |
| FT2 & FT3 [MN] | Mean | Maximum | Minimum | Standard deviation |
| DLW | 1.57 | 1.95 | 1.05 | 0.08 |
| DIEGO | 1.60 | 1.92 | 1.31 | 0.07 |
| HAWC2 | 1.49 | 1.73 | 1.24 | 0.06 |

where Fx: Tower bottom fore-aft force, My: Tower bottom overturning moment, FT1, FT2, and FT3: mooring #1, #2, and #3 tension force, respectively.

3.6. Turbulent wind cases

Two load cases considering turbulent wind were performed considering a mean wind speed at the hub height of 1) 8.32 m/s (below rated) for which the wind turbine is rotating at around 5.9 rpm and 2) 15.53 m/s (above rated) for which the wind turbine is rotating at around 7.53 rpm. Accordingly, the excitation frequencies correspond to the rotor frequency (1P), blade passing frequency (3P for three-bladed wind turbine) and the corresponding harmonics. The load cases are 700s long, from which the 200s first are regarded as transient and are removed from the analysis.

Figure 6 shows the evolution of the electrical power during both below and above rated turbulent wind load cases. Some differences can be noted between the three codes which may be due to a difference in the pitch servo control.



(a) Electrical power below rated wind speed

(b) Electrical power above rated wind speed

Figure 6: Electrical power curve comparisons below and above rated wind speed

The PSD of the tower fore-aft bending moment is shown in Figure 7. The rotor frequency, the blade passing frequency as well as the eigenfrequency of the tower are shown on the graph with vertical

dashed lines. The agreement between the three codes is very good. The three PSD depict the same peaks at the above-mentioned frequencies.

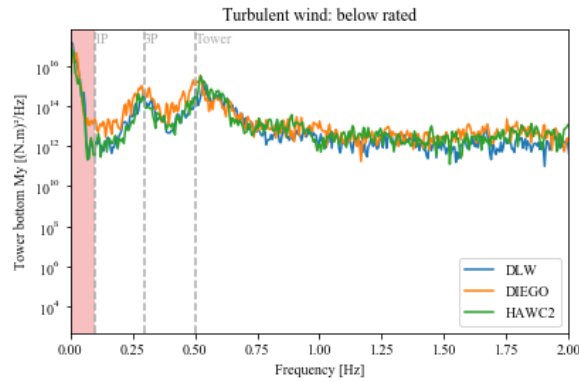


Figure 7: PSD of the fore aft bending moment at tower bottom (below rated turbulent wind load case)

Table 5 shows the statistics of quantities of interest of platform motion under turbulent wind inflow above rated wind speed. It shows a nice agreement between the three codes for the motions, except that DLW produces lower dynamic response in surge/sway/yaw than HAWC2 and DIEGO, as one can see from the standard deviations. The control strategy might be involved in this response. It seems also that the controller used in DIEGO increases a bit the excitation, resulting in slightly higher $F_x/My/Pitch$ responses.

Table 5: Basic statistics of quantities of interest during turbulent wind above rated load case

| surge [m] | Mean | Maximum | Minimum | Standard deviation |
|------------------------------|-------------|----------------|----------------|---------------------------|
| DLW | 15.08 | 17.78 | 13.28 | 1.18 |
| DIEGO | 14.91 | 18.79 | 10.00 | 2.12 |
| HAWC2 | 13.90 | 18.62 | 8.90 | 2.19 |
| sway [m] | Mean | Maximum | Minimum | Standard deviation |
| DLW | 0.48 | 1.70 | -1.22 | 0.73 |
| DIEGO | 1.15 | 6.96 | -3.56 | 3.08 |
| HAWC2 | -0.13 | 5.50 | -4.02 | 2.54 |
| heave [m] | Mean | Maximum | Minimum | Standard deviation |
| DLW | -0.09 | -0.04 | -0.14 | 0.02 |
| DIEGO | -0.08 | 0.00 | -0.15 | 0.03 |
| HAWC2 | -0.07 | 0.09 | -0.22 | 0.08 |
| roll [°] | Mean | Maximum | Minimum | Standard deviation |
| DLW | 0.59 | 1.15 | -0.17 | 0.27 |
| DIEGO | 0.55 | 1.33 | -0.30 | 0.29 |
| HAWC2 | 0.16 | 0.75 | -0.65 | 0.25 |
| pitch [°] | Mean | Maximum | Minimum | Standard deviation |
| DLW | 2.49 | 4.79 | 0.98 | 0.75 |
| DIEGO | 2.544 | 4.80 | 0.58 | 0.90 |
| HAWC2 | 2.43 | 4.30 | 1.14 | 0.62 |
| yaw [°] | Mean | Maximum | Minimum | Standard deviation |
| DLW | 2.06 | 5.23 | -1.08 | 1.48 |
| DIEGO | 0.79 | 5.26 | -4.26 | 2.52 |
| HAWC2 | 4.10 | 8.21 | -0.31 | 2.23 |
| F_x [MN] | Mean | Maximum | Minimum | Standard deviation |
| DLW | 1.32 | 2.17 | 0.76 | 0.23 |
| DIEGO | 1.31 | 2.25 | 0.34 | 0.31 |
| HAWC2 | 1.22 | 1.93 | 0.37 | 0.22 |

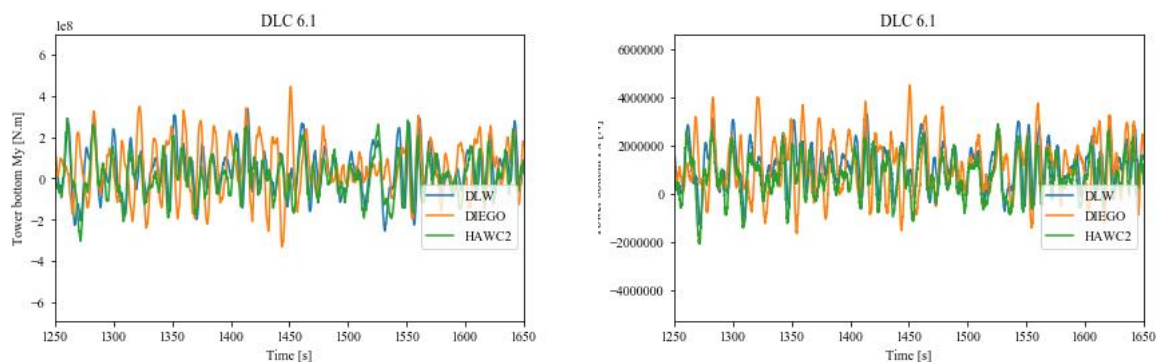
| My [MN.m] | Mean | Maximum | Minimum | Standard deviation |
|-----------|--------|---------|---------|--------------------|
| DLW | 202.69 | 402.65 | 83.42 | 53.41 |
| DIEGO | 215.65 | 385.08 | 43.44 | 65.95 |
| HAWC2 | 199.10 | 342.99 | 61.32 | 45.29 |

where F_x : Tower bottom fore-aft force, M_y : Tower bottom overturning moment, respectively.

3.7. Parked case

This load case consists in considering irregular ocean waves and a turbulent wind inflow at a mean wind speed of 50 m/s. The turbine is parked (i.e., blade pitch at 90° and the rotor is blocked). Figure 8 (a) and (b) show an extract of the time series between 1250 s and 1650 s of the bending moment and force at tower bottom. These figures show that there is a relatively good agreement among the three codes. This is also confirmed by the basic statistics of various quantities of interest presented in Table 6. In particular, it can be remarked:

- Despite some differences in the mean values, the surge, heave, and pitch dynamics are well aligned. In particular, HAWC2 provides the lowest mean surge because of low wave drag and mean horizontal force. When checking the larger value of the mean surge for DLW, it appears that this is related to a dynamic slack (i.e. loss of tension) along a mooring line, indicating that the model is not correctly designed for such extreme waves.
- Sway, roll and yaw dynamics are not really aligned, and each solver provides a different result. The same behaviour is obtained on mean values, leading to a poor global agreement on these degrees of freedom. The dynamic in roll, sway and yaw is stronger in DIEGO than in DLW and HAWC2. A detailed investigation will be performed as a future work.
- The forces at the tower bottom present a good agreement between HAWC2 and DLW, but DIEGO produces higher F_x ($\sim 30\%$ on the standard deviation) and overturning moment M_y ($\sim 20\%$ on the standard deviation) than HAWC2 and DLW, which are well aligned. Considering the results observed in the “wave only” case, it is probable that aerodynamics could cause this discrepancy.



(a) Extract of the tower bottom bending moment

(b) Extract of the tower bottom force

Figure 8: Tower bottom bending moment and force comparison

Table 6: Basic statistics of quantities of interest for the park condition

| surge [m] | Mean | Maximum | Minimum | Standard deviation |
|-----------|-------|---------|---------|--------------------|
| DLW | 16.37 | 26.96 | 9.03 | 2.42 |
| DIEGO | 15.65 | 24.27 | 8.10 | 2.64 |
| HAWC2 | 10.72 | 19.27 | 2.78 | 2.50 |
| sway [m] | Mean | Maximum | Minimum | Standard deviation |
| DLW | -7.06 | -3.67 | -10.89 | 1.36 |
| DIEGO | -1.26 | 11.18 | -17.15 | 6.70 |
| HAWC2 | 2.91 | 12.94 | -5.90 | 3.90 |

| heave [m] | Mean | Maximum | Minimum | Standard deviation |
|-----------------------------|-------------|----------------|----------------|---------------------------|
| DLW | 0.08 | 6.71 | -6.30 | 1.71 |
| DIEGO | 0.08 | 5.71 | -5.88 | 1.66 |
| HAWC2 | 0.12 | 4.71 | -4.24 | 1.43 |
| roll [°] | Mean | Maximum | Minimum | Standard deviation |
| DLW | 1.24 | 2.85 | -0.12 | 0.43 |
| DIEGO | 0.39 | 2.91 | -1.81 | 0.82 |
| HAWC2 | -0.25 | 1.11 | -1.81 | 0.52 |
| pitch [°] | Mean | Maximum | Minimum | Standard deviation |
| DLW | 0.37 | 4.22 | -3.59 | 1.09 |
| DIEGO | 0.56 | 4.44 | -3.31 | 1.13 |
| HAWC2 | 0.10 | 3.16 | -2.90 | 0.95 |
| yaw [°] | Mean | Maximum | Minimum | Standard deviation |
| DLW | 2.56 | 4.12 | 1.07 | 0.53 |
| DIEGO | 0.46 | 4.64 | -2.63 | 1.85 |
| HAWC2 | -0.73 | 1.46 | -2.55 | 0.75 |
| F_x [MN] | Mean | Maximum | Minimum | Standard deviation |
| DLW | 1.16 | 4.58 | -2.41 | 0.93 |
| DIEGO | 1.18 | 6.08 | -4.71 | 1.34 |
| HAWC2 | 0.72 | 4.77 | -2.83 | 0.91 |
| M_y [MN.m] | Mean | Maximum | Minimum | Standard deviation |
| DLW | 37.51 | 458.53 | -448.66 | 115.72 |
| DIEGO | 50.22 | 636.82 | -626.16 | 152.32 |
| HAWC2 | 10.28 | 371.16 | -334.17 | 104.04 |

where F_x : Tower bottom fore-aft force, M_y : Tower bottom overturning moment, respectively.

More detailed analysis results can be found from Ref. 10.

4. Conclusions

In this study, an extensive code-to-code comparison has been performed with three different numerical tools (DIEGO, DLW and HAWC2) with the modified IEA 15MW/UMaine floater to adapt to an offshore site in South Brittany (France) with 150m water depth. During the exercise, a redesign of the tower was realized to avoid the risk of resonance with a natural frequency too close to the 3P frequency.

In total 10 test cases were performed, among which 6 test cases were presented and discussed. When comparing the loads and motions both in time and frequency domains, generally good agreements are observed between the codes. However, some differences are noticed in specific degrees of freedom like roll, sway and yaw and for the surge with extreme waves. The latter indicates that the considered FOWT model is not well designed for the very extreme waves of the South Brittany site. A redesign of the mooring lines with clump weight has been conducted after this benchmark campaign. Detailed validation studies with the updated FOWT model will be conducted as future work. Furthermore, the aerodynamic loading influence for extreme wind parked configuration would require additional investigations.

5. Acknowledgements

This study was part of HIPERWIND project which has received funding from the European Union's Horizon 2020 Research and Innovation Programme under Grant Agreement No. 101006689.

The authors are also grateful to NREL and University of Maine for providing the initial design of the model. The authors also thank Y. Poirrette, V. Le Corre, T. Perdrizet, G. Gudendorff and V. Dupin of IFPEN for their support on the model settings and result interpretation

6. References

[1] European Commission, 2018. A Clean Planet for All

[2] <https://www.hiperwind.eu/>

[3] Allen, C., Viselli, A., Dagher, H., Groupee, A., Gaertner, E., Abbas, N., Hall, M., Barter, G. "Definition of the UMaine VoltturnUS-S Reference Platform Developed for the IEA Wind 15-Megawatt Offshore Reference Wind Turbine," Technical Report, NREL/TP-5000-76773, July 2020.

[4] <https://iea-wind.org/task30/>

[5] Evan Gaertner, Rinker, J., Sethuraman, L., Zahle, F., Anderson, B., Barter, G., Abbas, N., Meng, F., Bortolotti, P., Skrzypinski, W., Scott, G., Feil, R., Bredmose, H., Dykes, K., Sheilds, M., Allen, C., Viselli, A., "Definition of the IEA Wind 15-Megawatt Offshore Reference Wind Turbine," Technical Report, NREL/TP-5000-75698, March 2020.

[6] Larsen, T.J., Hansen, A.M., "How 2 HAWC2 the user's manual," Risø-R-1597 (ver. 12.9)(EN), 2021.

[7] Kim, T., Hansen, A.M., Branner, K., "Development of an anisotropic beam finite element for composite wind turbine blades in multibody system," *Renewable Energy*, 59, 2013, pp. 172–183.

[8] Madsen, H.A., Larsen, T.J., Pirrung, G.R., Li, A., Zahle, F., "Implementation of the blade element momentum model on a polar grid and its aeroelastic load impact," *Wind Energy Science* 2020, 5, 1–27. doi:10.5194/wes-5-1-2020.

[9] Le Cunff, C, Heurtier, JM, Piriou, L, Berhault, C, Perdrizet, T, Teixeira, D, Gilloteaux, JC, "Fully Coupled Floating Wind Turbine Simulator Based on Nonlinear Finite Element Method: Part I - Methodology," In ASME 2013 32nd International Conference on Ocean, Offshore and Arctic Engineering, 2013.

[10] <https://www.hiperwind.eu/publications>